Figures

Supplemental Figure 1

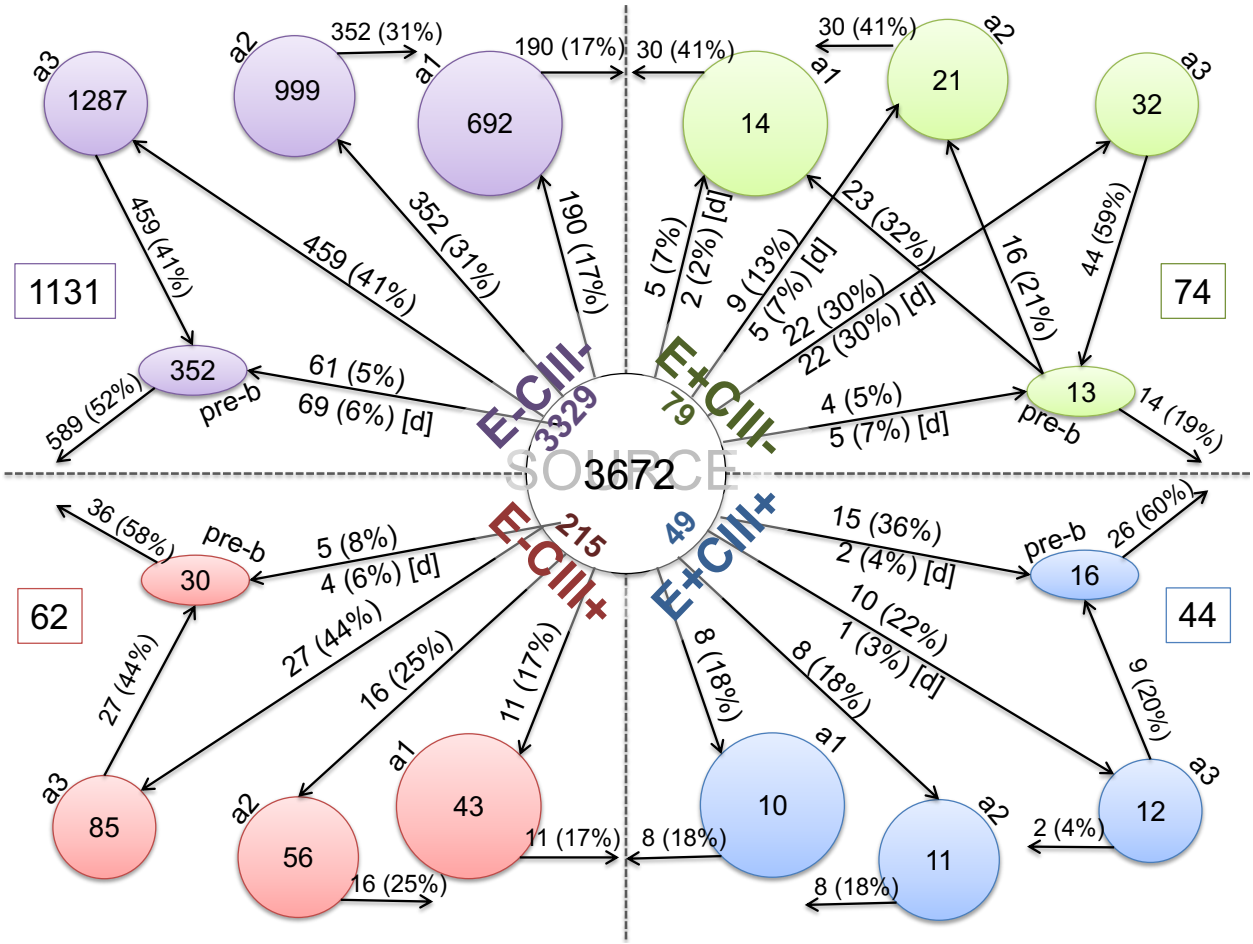

Supplemental Figure 1: Model-derived apoA-I flux rates and pool sizes across four HDL subspecies and sizes. Numbers inside the center circle (source compartment, representing liver or intestinal synthesis) represent apoA-I pool size for each subspecies and for total plasma. Numbers inside circles (HDL size compartments) represent mean pool size (mg). Numbers above lines represent mean flux in mg/day (% total flux for that subspecies). Numbers below lines with [d] = flux in mg/day (% of total flux for that subspecies) through intravascular delay compartments (not illustrated). Numbers in the colored boxes are total flux for that subspecies in mg/day. a1 = alpha-1; a2 = alpha-2; a3 = alpha-3, pre-b = prebeta

Supplemental Figure 2

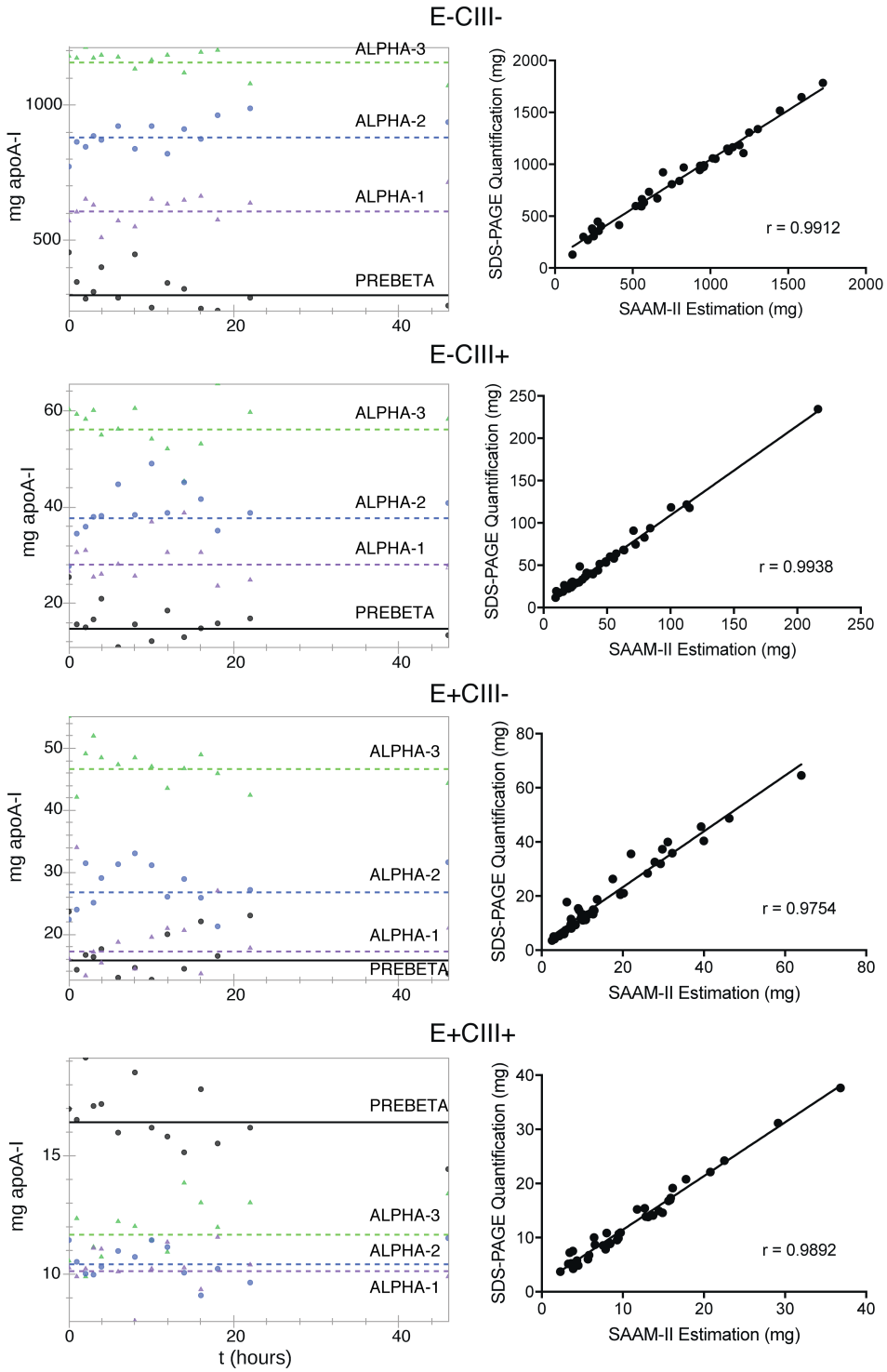

Supplemental Figure 2: Ability of SAAM-II to accurately estimate apoA-I pool sizes calculated from SDS-PAGE densitometry. Left: Mean apoA-I mass (pool size) model fits in SAAM-II for each HDL subspecies (by size). Right: Comparison of SAAM-II model estimation vs. SDS-PAGE quantification (right) for each subspecies (points = each HDL size of each study participant, 40 total per subspecies). Pearson correlation (r) shown. All SAAM-II estimations are within 1 standard deviation of mean SDS-PAGE quantification.

Tables

Supplemental Table 1: Fractional catabolic rates (pools/day) of apoA-I in four sizes of plasma HDL and in each HDL subspecies.

	Plasma ApoA-I (n=18)		E- (n=18)		E+ (n=18)		CIII- (n=10)		CIII+ (n=10)	
HDL Size	Mean	SEM	Mean	SEM	Mean	SEM	Mean	SEM	Mean	SEM
alpha-1	0.36	0.03	0.37	0.04	2.9	0.7	0.35	0.06	0.35	0.05
alpha-2	0.46	0.04	0.47	0.04	2.1	0.3	0.41	0.06	0.42	0.05
alpha-3	0.44	0.04	0.44	0.04	1.6	0.2	0.40	0.05	0.55	0.11
prebeta	3.7	0.66	4.4	0.90	6.9	1.4	2.7	0.51	1.7	0.28

Supplemental Table 2: Effect of covariates on FCRs, pool size, and secretion rates of apoA-I in HDL subspecies (n=10).

	Fractional catabolic rate (pools/day)[A]																	
	Sex				Race				ApoE Genotype						BMI (kg/m^2)			
	Male[B]		Female[C]		White[C]		Black[B]		E3/E3[B]		E4/E3[B]		E2/E4[D]		<30[E]		>30[E]	
HDL	Mean	SEM	Mean	SEM	Mean	SEM	Mean	SEM	Mean	SEM	Mean	SEM	Mean	SEM	Mean	SEM	Mean	SEM
E-CIII-	0.64	0.04	0.44	0.02	0.52	0.02	0.53	0.06	0.56	0.05	0.48	0.04	0.51	0.04	0.55	0.04	0.50	0.04
E-CIII+	0.60	0.09	0.47	0.04	0.57	0.07	0.46	0.05	0.54	0.02	0.54	0.10	0.48	0.05	0.51	0.02	0.54	0.09
E+CIII-	2.89	0.42	2.41	0.22	2.93	0.24	2.23	0.42	2.91	0.28	3.06	0.13	1.05	0.08	2.91	0.25	2.29	0.35
E+CIII+	1.57	0.34	1.06	0.26	1.56	0.35	0.82	0.09	1.33	0.28	1.44	0.36	0.77	0.10	1.72	0.35	0.81	0.12
	Plasma mass (mg)[F]																	
	Sex				Race				ApoE Genotype						BMI (kg/m^2)			
	Male		Female		White		Black		E3/E3		E4/E3		E2/E4		<30		>30	
HDL	Mean	SEM	Mean	SEM	Mean	SEM	Mean	SEM	Mean	SEM	Mean	SEM	Mean	SEM	Mean	SEM	Mean	SEM
E-CIII-	2967	101	3194	150	3038	162	3201	77	3336	170	2940	97	2965	1	3237	164	2970	84
E-CIII+	165	23	208	30	147	16	256	30	180	14	190	41	214	18	164	16	217	35
E+CIII-	59	10	71	10	45	4	98	8	53	4	61	12	105	2	50	4	83	11
E+CIII+	42	6	44	5	40	5	49	6	40	5	44	6	50	6	43	5	44	6
	Flux (mg/day)[G]																	
	Sex				Race				ApoE Genotype						BMI (kg/m^2)			
	Male		Female		White		Black		E3/E3		E4/E3		E2/E4		<30		>30	
HDL	Mean	SEM	Mean	SEM	Mean	SEM	Mean	SEM	Mean	SEM	Mean	SEM	Mean	SEM	Mean	SEM	Mean	SEM
E-CIII-	1922	172	1393	74	1530	55	1716	222	1870	176	1389	75	1504	118	1763	171	1446	98
E-CIII+	88	9	90	7	81	9	103	4	98	10	78	7	95	1	87	11	92	3
E+CIII-	138	20	168	27	129	14	198	31	160	22	177	30	109	6	150	21	163	28
E+CIII+	67	21	42	8	35	1	64	18	48	8	66	21	33	0	74	18	30	3

[A]FCRs for each HDL size are weighted by respective pool size and combined into a "total" FCR for each subspecies. [B]n=4. [C]n=6. [D]n=2. [E]n=5. [F]Pool sizes are calculated from SAAM-II. [G]Total amount cleared from plasma each day.

Supplemental Table 3: Concentrations[A] of apoE in HDL[B] that contains apoCIII and apoE in HDL that does not contain apoCIII, and Spearman correlations with apolipoproteins and triglycerides in the random subcohort, n=1750.

	Random subcohort (n=1,750)	CHD (n=1,946)	Random subcohort					
			ApoE in HDL		*ApoE in HDL that contains apoCIII*		*ApoE in HDL that does not contain apoCIII*	
			r	p	r	p	r	p
HDL-ApoA-I, mg/dL	136 (78, 224)	134 (74, 230)	0.160	<0.001	0.108	<0.001	0.137	<0.001
ApoCIII[C], mg/dL	11 (4, 23)	11 (4, 24)	0.040	0.098	0.153	<0.001	-0.039	0.100
ApoE in HDL, mg/dL	2 (1, 5)	2 (1, 7)						
ApoE in HDL that contains apoCIII, mg/dL	1 (0.2, 3)	1 (0.3, 4)						
ApoE in HDL that does not contain apoCIII, mg/dL	1 (0.3, 3)	1 (0.3, 3)						
HDL that contains apoCIII, mg/dL	11 (4, 26)	11 (4, 28)	0.064	0.007	0.149	<0.001	-0.001	0.976
HDL that does not contain apoCIII, mg/dL	123 (71, 202)	122 (67, 211)	0.162	<0.001	0.094	<0.001	0.145	<0.001
ApoB, mg/dL	88 (48, 146)	98 (54, 167)	-0.069	0.004	0.018	0.453	-0.113	<0.001
Triglycerides, mg/dL	81 (36, 237)	108 (43, 304)	0.021	0.373	0.193	<0.001	-0.133	<0.001

[A]Median (5th and 95th percentiles). [B]The concentration of HDL was quantified based on apoA-I levels, the major apolipoprotein component of HDL. [C]n=1749.

Supplemental Table 4: Hazard Ratios (HRs)[A] and 95% confidence intervals of CHD according to quintiles of the concentration of apoE in unfractionated HDL[B] or the concentration of apoE in HDL subspecies in participants of the Danish Diet Cancer and Health study, n=3639.

	Q1	Q2	Q3	Q4	Q5	P trend	Per $\log_2$ increase[C]	P heterogeneity[D]
ApoE in HDL								
Median levels in sub-cohort, mg/dL	0.93	1.48	1.95	2.67	4.27			
Number of CHD cases	352	359	378	390	467			
Unadjusted	1 (ref)	0.90 (0.69, 1.19)	0.82 (0.61, 1.09)	0.83 (0.62, 1.12)	0.91 (0.65, 1.28)	0.81	0.95 (0.83, 1.08)	
Multivariable-adjusted[E]	1 (ref)	0.99 (0.74, 1.33)	0.92 (0.67, 1.26)	0.91 (0.67, 1.25)	0.97 (0.66, 1.41)	0.88	0.93 (0.81, 1.08)	
Plus HDL	1 (ref)	1.01 (0.75, 1.36)	0.94 (0.68, 1.29)	0.95 (0.69, 1.31)	1.07 (0.73, 1.56)	0.71	0.97 (0.84, 1.13)	
Plus HDL and apoCIII[F]	1 (ref)	0.99 (0.74, 1.34)	0.90 (0.66, 1.25)	0.90 (0.65, 1.25)	0.97 (0.66, 1.42)	0.88	0.93 (0.80, 1.08)	
Plus HDL, apoCIII, triglycerides, apoB[G]	1 (ref)	0.99 (0.73, 1.33)	0.86 (0.62, 1.19)	0.88 (0.63, 1.21)	0.94 (0.63, 1.38)	0.79	0.90 (0.77, 1.05)	
ApoE in HDL that contains apoCIII								
Median levels in sub-cohort, mg/dL	0.31	0.53	0.75	1.03	1.86			
Number of CHD cases	256	249	316	437	688			
Unadjusted	1 (ref)	1.07 (0.80, 1.44)	1.19 (0.86, 1.64)	1.31 (0.94, 1.82)	1.40 (0.96, 2.03)	0.08	1.14 (1.00, 1.29)	0.01
Multivariable-adjusted[E]	1 (ref)	1.02 (0.74, 1.41)	1.16 (0.82, 1.64)	1.34 (0.94, 1.91)	1.29 (0.86, 1.93)	0.25	1.12 (0.98, 1.28)	0.02
Plus HDL	1 (ref)	1.03 (0.75, 1.42)	1.18 (0.83, 1.67)	1.37 (0.96, 1.95)	1.32 (0.88, 1.97)	0.22	1.13 (0.99, 1.29)	0.03
Plus HDL and apoCIII[F]	1 (ref)	0.99 (0.71, 1.36)	1.11 (0.78, 1.57)	1.24 (0.86, 1.78)	1.16 (0.77, 1.76)	0.54	1.08 (0.94, 1.24)	0.05
Plus HDL, apoCIII, triglycerides, apoB[G]	1 (ref)	0.94 (0.68, 1.30)	1.00 (0.70, 1.42)	1.09 (0.76, 1.58)	1.02 (0.67, 1.55)	0.86	1.03 (0.89, 1.18)	0.18
ApoE in HDL that does not contain apoCIII								
Median levels in sub-cohort, mg/dL	0.44	0.72	1.00	1.40	2.19			
Number of CHD cases	416	407	358	341	424			
Unadjusted	1 (ref)	0.84 (0.64, 1.10)	0.79 (0.60, 1.04)	0.61 (0.46, 0.82)	0.66 (0.49, 0.89)	<0.01	0.88 (0.79, 0.98)	
Multivariable-adjusted[E]	1 (ref)	0.77 (0.58, 1.02)	0.79 (0.59, 1.05)	0.63 (0.46, 0.85)	0.66 (0.48, 0.89)	0.01	0.88 (0.78, 0.98)	
Plus HDL	1 (ref)	0.78 (0.59, 1.03)	0.79 (0.59, 1.06)	0.64 (0.47, 0.88)	0.70 (0.51, 0.96)	0.03	0.90 (0.80, 1.01)	
Plus HDL and apoCIII[F]	1 (ref)	0.78 (0.59, 1.04)	0.80 (0.60, 1.07)	0.64 (0.47, 0.88)	0.68 (0.49, 0.93)	0.02	0.89 (0.79, 1.00)	

Plus HDL, apoCIII, triglycerides, apoB[G]	1 (ref)	0.80 (0.60, 1.06)	0.80 (0.59, 1.07)	0.68 (0.50, 0.93)	0.68 (0.49, 0.94)	0.02	0.90 (0.80, 1.01)

[A]Hazard Ratios (HRs) obtained from Cox proportional hazard regression models with age used as the underlying time scale, adjusted for laboratory batch and stratification by sex.

[B]The concentration of HDL was quantified based on apoA-I levels, the major apolipoprotein component of HDL.

[C]Equivalent to doubling in apoE.

[D]We tested for equality of the regression coefficients for apoE in HDL containing apoCIII and apoE in HDL not containing apoCIII (p heterogeneity).

[E]ApoE in HDL containing or not containing apoCIII are simultaneously included in all models. The multivariable model was adjusted for laboratory batch, smoking status (never; former; current <15, 15-24, ≥ 25 g/day), education (missing, <8; 8-10; >10 years), alcohol intake (nondrinker; drinker <5, 5-9, 10-19, 20-39, ≥40 g/alcohol/day), BMI (<25; 25-<30; >30 kg/m^2), and self-reported diagnosis of hypertension, and self-reported diagnosis of diabetes at baseline.

[F]n=3638. [G]n=3635

Supplemental Methods: Kinetic model development.

TABLE OF CONTENTS

PART 1: Establishing final models

All compartmental modeling was performed using SAAM-II (The Epsilon Group, Charlottesville, VA). Various models were tested and examined for visual and statistical fits. For all models, the input/forcing function was free plasma leucine d3 enrichment.

Because the canonical stepwise enlargement model is not a good fit for human HDL apoA-I kinetic data (main text ref. 41), and the tracer enrichment curves in the present study were not compatible with a major precursor-product relationship between prebeta HDL and alpha HDL, we began model testing with the published Mendivil et al. model (41). The MENDIVIL MODEL was optimized for plasma apoA-I on HDL without separating into apolipoprotein-based subspecies. It is characterized by direct secretion of all HDL sizes and certain size conversion pathways, as shown below:

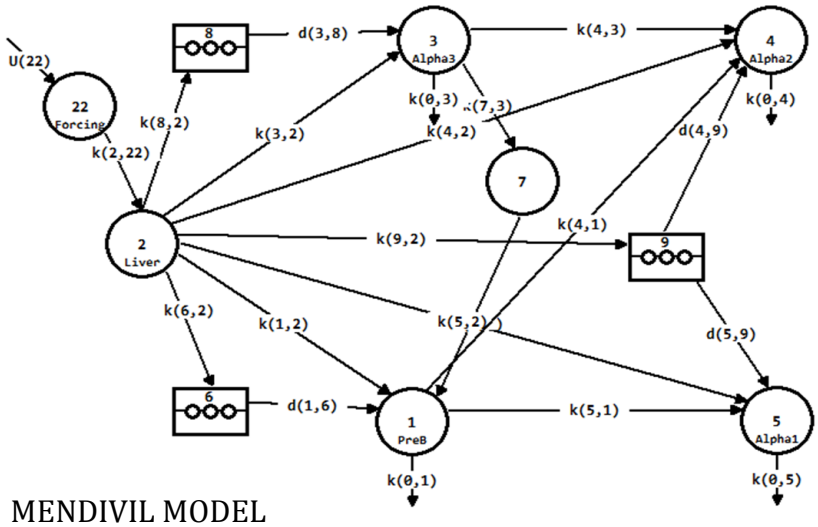

MENDIVIL MODEL

The model fits to the tracer enrichment curves were visually satisfactory for most subspecies and sizes, as shown below:

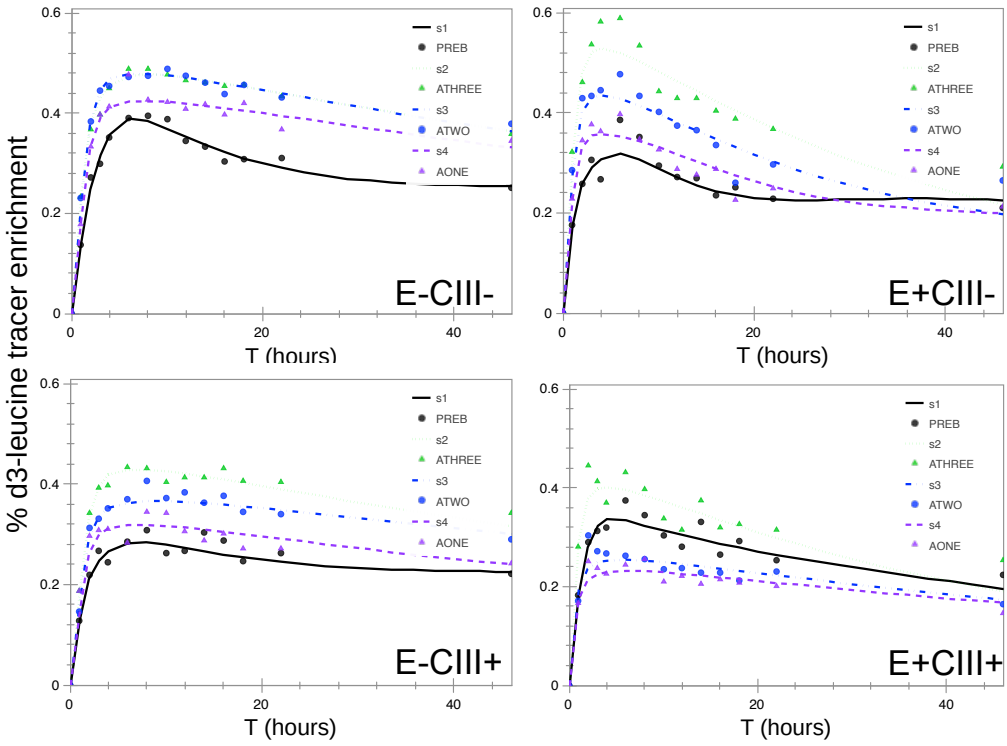

However, there were a few aspects of the MENDIVIL MODEL that warranted further optimization: several parameters hit lower limits (zero) depending on the subspecies, suggesting redundancy and over-parameterization; the delay times were often very small, leading us to question if they were necessary; coefficients of variance for many parameters were over 50%, meaning that the modeling software was not precisely estimating them. Given that over-parameterization was the main concern, we removed the delay compartments to alpha-1, -2 and -3 since they were all <1 hour. We assessed the need for size expansion pathways for E-CIII-, the major subspecies, by creating a model that is primarily defined by direct secretion and clearance of all sizes of HDL (MINIMUM MODEL):

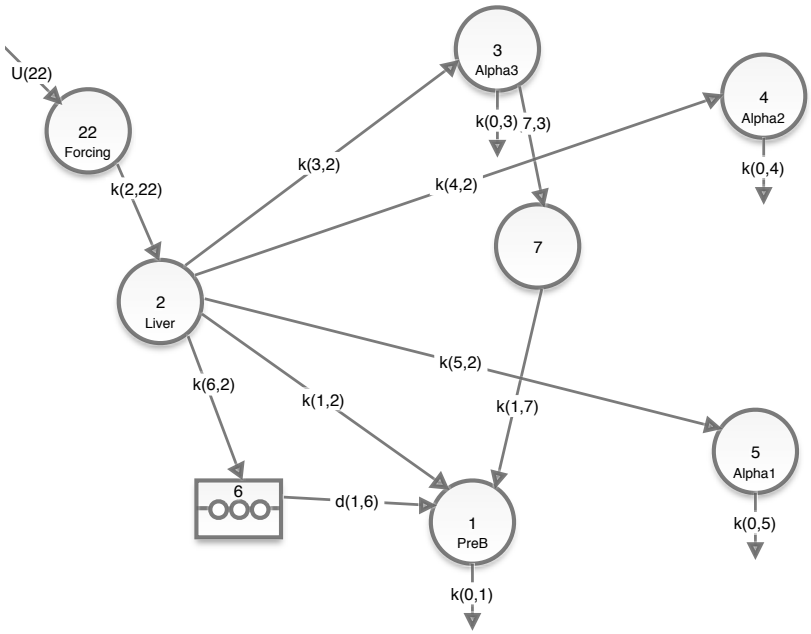

The "**minimum model**" is characterized by direct secretion of all HDL sizes from the source compartment (here labeled as "liver," but also representing intestinal lipoprotein synthesis), an intravascular remodeling compartment for prebeta (the box labeled "6"), size contraction from alpha-3 to prebeta (the circle labeled "7"), and direct clearance of all HDL sizes. Plasma leucine enrichment is modeled as a forcing function.

The fits for the MINIMUM MODEL are shown below:

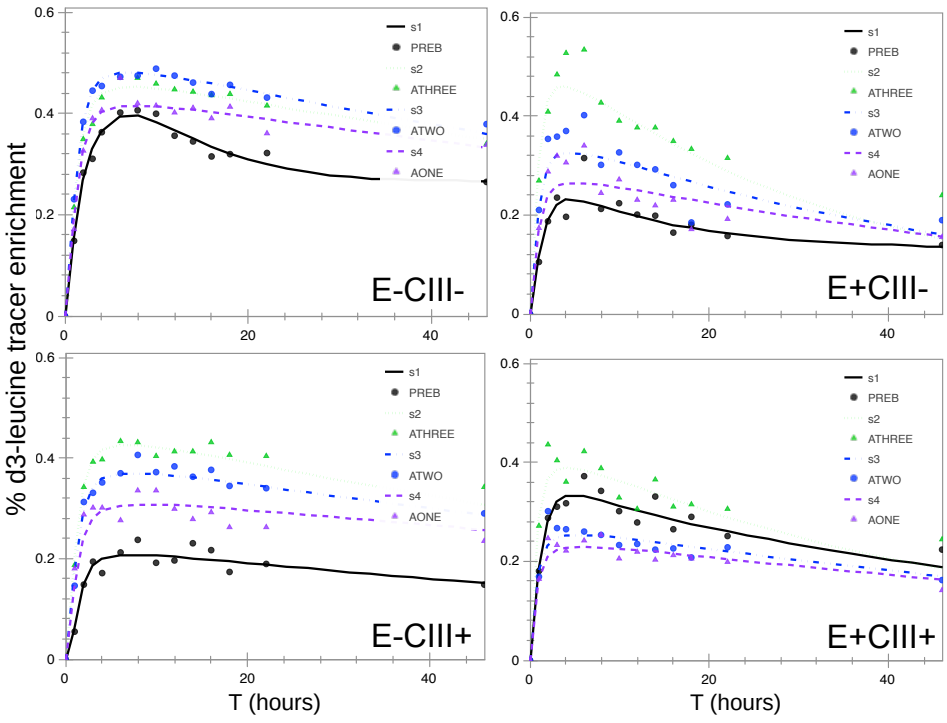

The MINIMUM MODEL visually fit the major HDL fraction E-CIII-, failed to fit the complex behavior of E+CIII-, and fit but had unused parameters in E-CIII+ and E+CIII+. We chose to focus first on finalizing the model for E-CIII-, the major HDL subspecies, to use it as an example for the other subspecies.

The next phase of modeling was to check the model for statistical precision. SAAM-II modeling software provides parameter standard deviations, coefficients of variation (CV), and 95% confidence intervals after every attempt at solving. The CV gives a judgment of the error associated with estimating the parameter, relative to the value of the parameter. For the normal distribution, about 95% of the values fall within 2 standard deviations of the set, so a CV of 50% corresponds to a 95% confidence interval with a lower limit approximately equal to zero. Thus, if a parameter value has a CV less than 50%, the 95% confidence interval excludes zero, and the pathway can be assumed to be real. In some cases, the CVs are reported to be well above 100%, which can be a clue that a parameter is unnecessary in the model. For example, the E-CIII- model parameters after running the final MINIMUM MODEL were as follows:

Parameter	Value (pools/hr)	Std. Dev.	Coef. of Var. (%)	95% Confidence Interval	
INPUT	37.14	12.54	33.77	12.22	62.06
delay6	3.30	6.95	210.54	-10.51	17.11
k(0,1)	0.05	0.10	188.73	-0.14	0.25
k(0,3)	0.00	0.03	**986.58**	-0.05	0.05
k(0,4)	0.01	0.01	38.40	0.00	0.02
k(0,5)	0.01	0.00	38.11	0.00	0.02
k(1,2)	0.10	0.03	33.85	0.03	0.17
k(1,7)	0.04	0.04	100.36	-0.04	0.11
k(2,22)	11.66	1.20	10.25	9.29	14.04
k(3,2)	0.54	0.18	33.35	0.18	0.90
k(4,2)	0.44	0.15	33.35	0.15	0.73
k(5,2)	0.26	0.09	33.77	0.09	0.43
k(6,2)	0.05	0.10	207.68	-0.16	0.26
k(7,3)	0.01	0.03	251.97	-0.04	0.06

The **k(0,3)** parameter, representing the rate constant for removal of alpha-3 HDL from circulation, had a CV of 987%. Deleting this pathway did not significantly alter the

FCRs, but made all other parameter estimates more accurate, even the ones not associated with alpha-3 or prebeta (see below).

Parameter	Value (pools/hr)	Std. Dev.	Coef. of Var. (%)	95% Confidence Interval	
INPUT	37.21	12.52	33.64	12.34	62.08
delay6	3.73	4.20	112.71	-4.62	12.08
k(0,1)	0.06	0.02	36.97	0.02	0.11
k(0,4)	0.01	0.01	38.23	0.00	0.02
k(0,5)	0.01	0.00	37.95	0.00	0.02
k(1,2)	0.10	0.03	30.80	0.04	0.16
k(1,7)	0.04	0.03	85.85	-0.03	0.10
k(2,22)	11.74	0.70	5.99	10.34	13.14
k(3,2)	0.54	0.17	32.02	0.20	0.88
k(4,2)	0.44	0.14	32.14	0.16	0.72
k(5,2)	0.26	0.08	32.61	0.09	0.42
k(6,2)	0.06	0.05	75.08	-0.03	0.15
k(7,3)	0.01	0.00	38.04	0.00	0.02

FCR (pools/day)				
	alpha-1	alpha-2	alpha-3	prebeta
With k(0,3)	0.27	0.32	0.30	1.26
Without k(0,3)	0.27	0.32	0.30	1.51

Removing this parameter directs all of the alpha-3 apoA-I into a processing compartment representing HDL that is remodeling to eventually become prebeta HDL. The only remaining parameters with high CVs are associated with non-sampled compartments (the prebeta delay compartment between source and plasma (Compartment 6) and the "remodeling" compartment connecting alpha-3 to prebeta (Compartment 7). We termed this model the "BARE MINIMUM MODEL" based on its parsimony.

The model fits were virtually superimposable, regardless of the presence of **k(0,3)**:

With k(0,3) (MINIMUM MODEL)	Without k(0,3) (BARE MINIMUM MODEL)
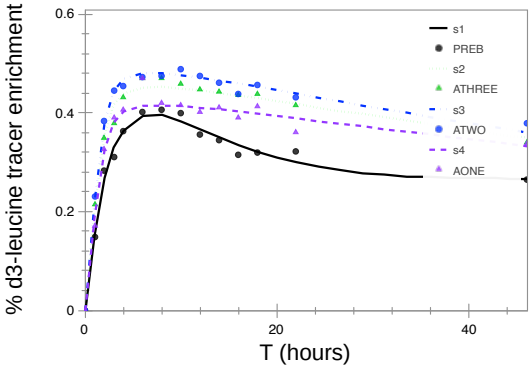	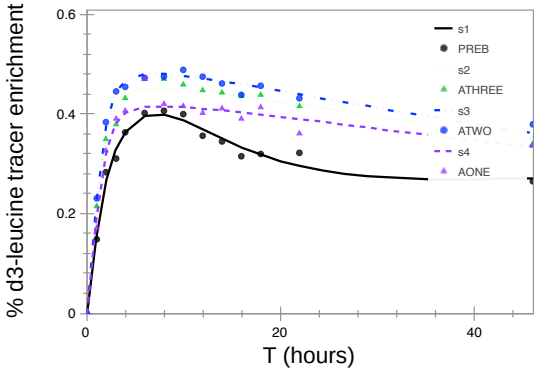

We also considered the possibility that prebeta did not need the "remodeling" compartment at all, and deleted it from the model while keeping **k(0,3)** (required to give alpha-3 HDL a removal mechanism and to maintain steady state). However, the prebeta fit was poor, leading us to conclude that the non-sampled "prebeta remodeling" compartment was absolutely necessary to fit the complex behavior of the prebeta size fraction:

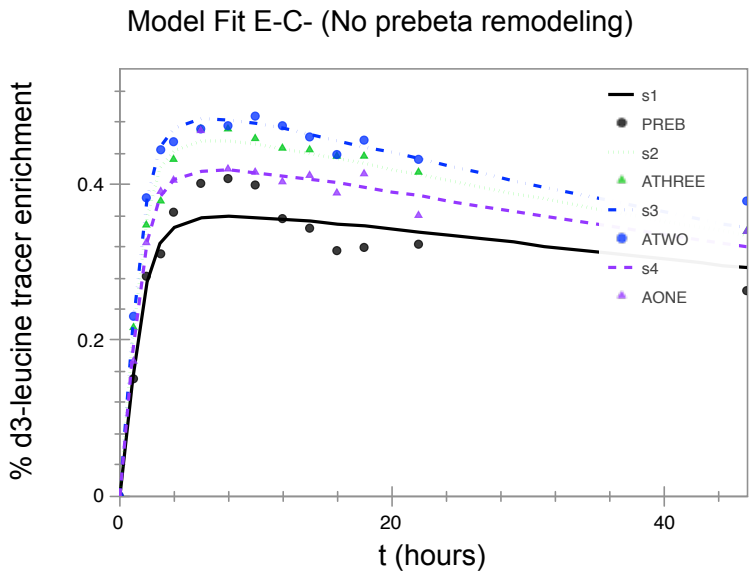

We next considered the possibility that, although the "prebeta remodeling" compartment was necessary to fit prebeta, it did not necessarily have to come from alpha-3. We tested this compartment (grey circle) originating from alpha-1 or alpha-2 along with keeping or removing (red "X") the direct clearance arrows:

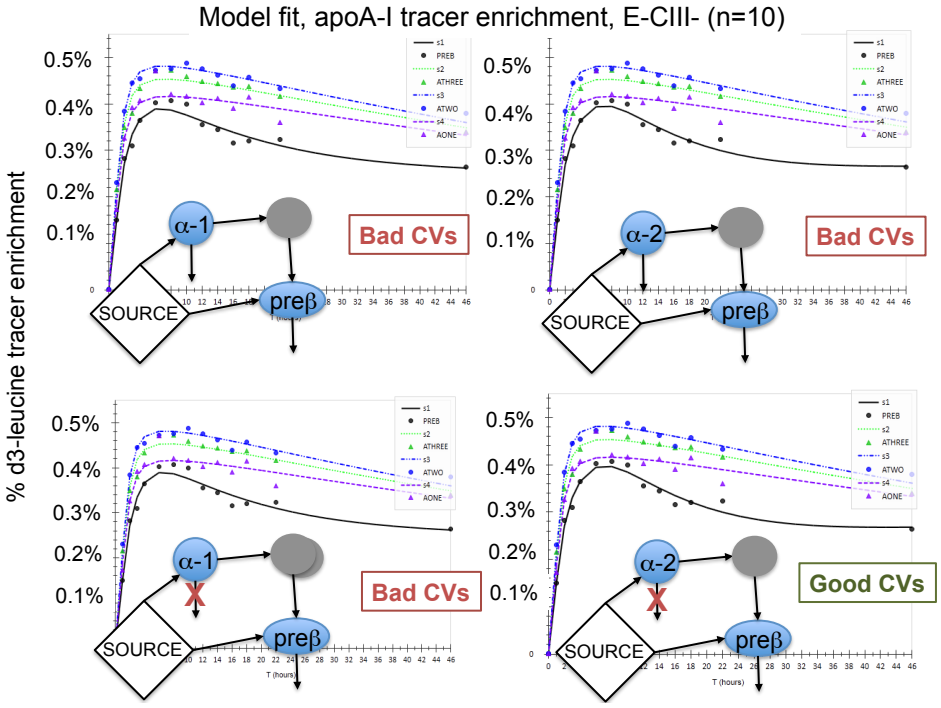

Although the visual fits were all similar, the only combination that had acceptable CVs was the "prebeta precursor" compartment originating from alpha-2 without an extra removal pathway for alpha-2 (bottom right corner). Upon comparing the MINIMUM MODEL to the model in which the "prebeta precursor" compartment came from alpha-2 or alpha-3, the results show that both models are visually identical and give nearly identical rate constants:

FCR (pools/day)				
	alpha-1	alpha-2	alpha-3	prebeta
Minimum model	0.27	0.32	0.30	1.26
From alpha-2	0.27	0.32	0.30	1.27
From alpha-3	0.27	0.32	0.30	1.51

Thus, we could not resolve the differences between the two origin pathways. We did not find evidence in the literature to support alpha-2 converting to prebeta, and kept the

remodeling compartment originating from alpha-3 HDL; the model is shown in **Figure 3A**, the BARE MINIMUM MODEL. This model gave a satisfactory fit except for E+CIII-. For this subspecies, we tested size expansion pathways from prebeta to alpha-1 and alpha-2 (schematic shown in **Figure 3B**). These model fits (**Figure 6A**) are visually superior to the fits from the MENDIVIL MODEL, especially in regards to hitting the final time points. Additionally, the size expansion pathways were successful in capturing the complex behavior of the E+CIII- fraction, though some of the peak time points were not completely reached by the model. However, fitting these points manually would require extremely high (and physiologically implausible) FCRs. This model provided the lowest sum of squared residuals because it captured later timepoints very well. We confirmed this by exporting the values for the weighted residuals at each time point for each HDL size, squaring them, and summing them (Weighted Residual Sum of Squares, WRSS). By F test, which rewards parsimony, the more complex model reduced the WRSS substantially enough to justify the additional parameters (**Figure 7**).

The modeling for individual participants begins once a model for a given subspecies has been chosen that has a full cassette of low-CV parameters. This involves loading the "final" model to the PopKinetics program, a component of SAAM-II. Study subject files are specified and the program fits the model to the data for each individual subject. Population-wide parameter values and statistics are given at the end of the iterations. Errors generally occur when parameters hit upper and lower limits. A lower limit can indicate that a certain metabolic pathway is not compatible with the data. Upper limits may be physiologically implausible (i.e. 20 pools/hour) and demonstrate that the program cannot fit the data to the given model. In either case, the program skips the subject and moves on to the next one. The entire process takes several iterations of PopKinetics solving with manual review and optimization of each participant's data.

In some cases, we removed outlier points to improve the fit. Outliers in the middle of the time range are not considered "high leverage" (their inclusion, or removal, has no effect on the model prediction) and were generally not removed. However, observations at the earliest and latest time points have a lot of leverage and can skew the fit or cause errors in fitting. Because there were several early time points in the initial ascending slope of the enrichment curve, an outlier in this zone was removed if it did not follow the

general trend of the rest of the data. However, the latest time point was always included unless it led to convergence errors in solving, because it was the only time point at that end.

We also used Bayesian estimation to improve parameter estimation. From the SAAM-II manual: *"The SAAM II Bayesian feature allows the incorporation of prior knowledge of the model parameters into the modeling of the kinetic data. The additional information is entered as a mean and standard deviation for one or more of the parameters in the model. The values can come from previous individual experiments, analysis of a population, or from published results."* In this case, we used parameter means and standard deviations from the model results using the mean enrichment and mass data of the all study participants. Bayesian estimation was only used for estimating rate constants involved in calculating fractional catabolic rates, which show more consistency across individuals than do rate constants involved in secretion pathways.

The individual modeling process concludes when all of the parameter CV's are below 50%. Exceptions are made for parameters associated with non-sampled pools (delays and the "prebeta precursor" compartment), which are more difficult to fit with precision.

PART 2: Individual Variation in Models

For each subspecies, we sought a single model that was able to describe the apoA-I metabolism of all study participants; however, some subspecies had variation in the models that best fit each participant. This was only an issue in the E+CIII+ and E+CIII- subspecies (and their parent subspecies, E+).

E+CIII+: The most common variant was removal of the delay compartment for prebeta secretion. Additionally, two participants needed a delay compartment for alpha-3, which had a more complex shape than the bare minimum model could accommodate. We also removed the prebeta remodeling compartment in two participants due to extraordinarily high CVs and convergence errors when solving the model.

E+CIII-: The best model for the mean enrichment and mass data featured size expansion from prebeta to alpha-1 and alpha-2. Individually, there was some variation in

the type of size expansion. Out of 10 participants, 9 required size expansion pathways in the model to visually fit the data and improve the model statistics. Of the 9 participants with size expansion, five had both pathways (from prebeta to alpha-1 and to alpha-2), and four only had size expansion to alpha-1. For the participants with size expansion, we modeled them using both the BARE MINIMUM MODEL and complex model (BARE MINIMUM MODEL plus size expansion) for comparison with an F test. The formula for calculating F is:

$$F = \frac{(WRSS_1 - WRSS_2)(N - P_2)}{WRSS_2(P_2 - P_1)}$$

Where WRSS is the weighted residual sum of squares, N is the number of data points, and P is the number of model parameters. The subscript "1" indicates the simpler model. The test has a Fisher distribution with (P_2-P_1, N-P_2) degrees of freedom (df). The results are shown below, demonstrating that the complex model was justified in its additional parameters in nine out of ten individuals given its significant reduction in WRSS:

ID	WRSS1	P1	WRSS2	P2	N	F	df1	df2	Fcrit	Reject?	p value
227	6.85	13	6.82	15	54	0.10	2	39	3.24	no	0.90
233	8.95	13	6.42	16	54	4.99	3	38	2.85	yes	0.005
243	28.85	13	13.70	17	54	10.22	4	37	2.63	yes	0.00001
244	20.05	13	12.17	16	52	7.77	3	36	2.87	yes	0.0004
248	8.37	13	4.70	17	51	6.63	4	34	2.65	yes	0.0005
250	10.36	13	6.55	16	50	6.60	3	34	2.88	yes	0.0012
268	19.60	13	13.41	16	53	5.69	3	37	2.86	yes	0.003
282	10.76	13	7.85	16	52	4.45	3	36	2.87	yes	0.009
286	8.17	13	6.51	15	53	4.83	2	38	3.24	yes	0.014
296	27.42	13	16.98	16	50	6.97	3	34	2.88	yes	0.0009

F tests are more useful for comparing models than the Aikake Information Criterion (AIC) or Bayes Information Criterion (BIC), which do not have distributions and thus cannot be statistically compared.

HDL containing apoE (**Figure 2**): There was variation in the extent of size expansion among study participants. Additional size expansion pathways, which

improved visual fit and model statistics, were used in only half (9/18) of the participants' models. This likely reflects antagonism by apoCIII also present in this subspecies. Of the nine that did have size expansion pathways from prebeta, four had expansion only to alpha-1, two had expansion only to alpha-2, and three had both pathways (from prebeta to alpha-1 and to alpha-2).

PART 3: Testing other hypotheses

A guiding principle of modeling is parsimony – to find the simplest model that can explain the data. However, there were certain aspects of biology that we wanted to test: size expansion in HDL not containing apoE and conversion of HDL subspecies.

Size expansion in HDL not containing apoE: Though the focus of our study was to test the effects of apoE and apoCIII on apoA-I metabolism, there are many other proteins present on HDL that could also be participating in classical reverse cholesterol transport. These proteins are generally present at minor amounts on HDL particles, but their influence could be quantifiable. Thus, though we described the metabolism of apoA-I on HDL not containing apoE using the BARE MINIMUM MODEL (**Figure 3A**), we also tested size expansion in HDL not containing apoE. In this subspecies, size expansion was occurring in 4/18 participants, accounting for an average of 6% of total flux in those participants. Other proteins present in E- are presumably acting to cause this size expansion. However, given that they probably comprise only 1-5% of the mass of HDL, their effects are probably being masked. We also tested the E-CIII+ subspecies to see if apoCIII was promoting size expansion in the absence of apoE. In E-CIII+, 5/10 people showed size expansion of some kind. However, size expansion pathways did not improve any of the visual fits or parameter CVs, so we used the BARE MINIMUM MODEL for all kinetic analyses in these subspecies.

Transfer of apoA-I between subspecies: It is possible that apoA-I can move between subspecies (or, equivalently, that HDL could gain or lose apoE or apoCIII). For example, as this occurs, an E+CIII- HDL could become an E-CIII- if all apoE molecules are lost; or it could become an E+CIII+ if apoCIII is acquired. To see if we had any evidence of conversion of one subspecies to another, we examined all possible

combinations of the tracer enrichment curves of each HDL size to assess evidence of precursor-product relationship between any two subspecies. Precursor-product evidence could suggest, but not confirm, that apoA-I is moving between subspecies (or, equivalently, that HDL is gaining or losing apoE or apoCIII). A subspecies change requires acquisition of at least one molecule of or complete loss of apoCIII or apoE. An example for the alpha-3 size is shown below:

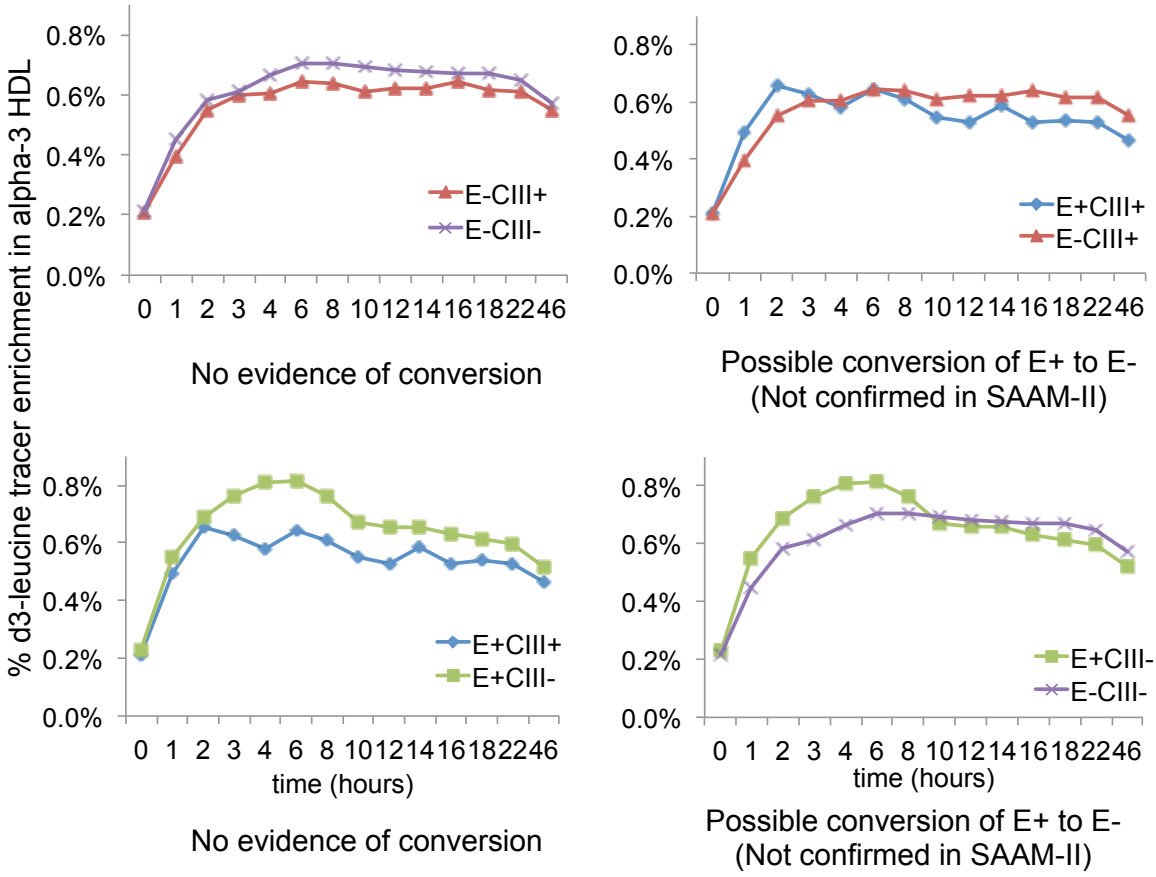

The enrichment curves for CIII+ and CIII- holding apoE constant (left panels) were parallel over the entire study period, providing no evidence of conversion of apoA-I HDL from CIII+ to CIII- HDL or vice versa. The enrichment curves for E+ and E- holding apoCIII constant (right panels) were compatible with some conversion of an E+ HDL subspecies to an E- subspecies. We tested models that included a transfer pathway from an E+ to an E- subspecies. The rate constants for this pathway hit zero, thus not confirming the existence of this pathway. Conversion of an E+ to an E- subspecies could

occur only if all apoE molecules left an HDL E+ particle. However, a small amount of loss of apoCIII or apoE from E+ or CIII+ that does not produce a subspecies change would not be recognized in this system. Finally, because the enrichment curves are compatible with conversion of E+ to E-, but not with acquisition of apoE by E- HDL, any apoE leaving the HDL could not be moving to E- HDL.